Journal of Power Sources 194 (2009) 1135–1141

Contents lists available at ScienceDirect

Journal of Power Sources

journal homepage: www.elsevier.com/locate/jpowsour

Paper-based, printed zinc–air battery

M. Hilder[a], B. Winther-Jensen[b], N.B. Clark[a,*]

[a] CSIRO Materials Science and Engineering, Private Bag 10, Clayton South, 3169 Victoria, Australia
[b] Materials Engineering, Monash University Clayton, 3800 Victoria, Australia

ARTICLE INFO

Article history:
Received 17 March 2009
Received in revised form 25 May 2009
Accepted 12 June 2009
Available online 24 June 2009

Keywords:
Batteries
Zinc
Conducting polymers
Poly(3,4-ethylenedioxythiophene) (PEDOT)
Inkjet printing
Carbon

ABSTRACT

A flexible battery is printed on paper by screen-printing a zinc/carbon/polymer composite anode on one side of the sheet, polymerising a poly(3,4-ethylenedioxythiophene) (PEDOT) cathode on the other side of the sheet, and applying a lithium chloride electrolyte between the two electrodes. The PEDOT cathode is prepared by inkjet printing a pattern of iron(III)*p*-toluenesulfonate as a solution in butan-1-ol onto paper, followed by vapour phase polymerisation of the monomer. The electrolyte is prepared as a solution of lithium chloride and lithium hydroxide and also applied by inkjet printing on to paper, where it is absorbed into the sheet cross-section. Measurements on a zinc/carbon-PEDOT/air battery in a similar configuration on a polyethylene naphthalate substrate shows a discharge capacity of up to 1.4 mAh cm^{-2} for an initial load of 2.5 mg zinc, equivalent to almost 70% of the zinc content of the anode, which generates 0.8 V at a discharge current of 500 μA. By comparison, the performance of the paper-based battery is lower, with an open-circuit voltage of about 1.2 V and a discharge capacity of 0.5 mAh cm^2. It appears that the paper/electrolyte combination has a limited ability to take up anode oxidation products before suffering a reduction in ionic mobility. The effects of different zinc/carbon/binder combinations, differences in application method for the zinc/carbon composite and various electrolyte compositions are discussed.

1. Introduction

Previous work by our group has focused on the development of printable smart packaging devices, based on electrochromic polypyrrole (PPy) [1], or dye release from within PPy and PEDOT (poly(3,4-ethylenedioxythiophene)) films [2]. These and most other printed electronic devices may require metal components to function as designed, for example, self-powered devices [3] may incorporate electrochemical cells with electrodes to provide electrical potentials to other parts of the device. Further, the recent finding that PEDOT can be used as a very efficient air-electrode material [4,5] combined with the printability of PEDOT [2] makes this material an obvious candidate for cathodes in low-cost, metal–air batteries.

The economic viability of the above devices depends on the rapid and low-cost application of metals to flexible substrates. The advantages of applying metals in a controlled manner without the usual engineering methods (cut-and-place assembly, electrolytic deposition, welding, soldering, etc.) are compelling and generally acknowledged in the literature. Very often, printing is considered to be the most attractive alternative that builds on conventional and well-understood technologies suitable for high-volume, low-value applications. Enquiries within the ink manufacturing industry [6] suggested that whilst conducting inks are readily available using noble metals such as silver, those based on galvanic metals such as aluminium, magnesium or zinc are less common. Although most silver-coloured inks use aluminium flakes in their formulation to give high lustre, concentrations are generally too low to overcome the insulating properties of the ink resins employed. Zinc-based epoxy paints are widely available as anti-corrosion treatments for steelwork but our preliminary tests have shown that these coatings do not provide a galvanic film suitable for the intended requirements.

The most common objective in printing metals is to apply a simple conducting pathway suitable for use as an electrical circuit. This objective often does not include the need for application to flexible substrates such as plastic films and papers. Accordingly, several processes have been previously devised that include post-treatment (thermal curing, electron beam curing, or photo curing) following deposition. The purpose of this treatment is to modify or remove binders, stabilisers and dispersants that would otherwise interfere with conduction between metal particles in the deposit. Similarly, other methods exist in which oxides are deposited and then an annealing step at high temperature used in combination with reducing agents to convert the oxide to the corresponding metal [7]. Clearly, high-temperature processes are inappropriate for smart packaging applications, not only because of the likely cost of the energy required for high-volume production, but also because paper and plastic packaging substrates typically show little tolerance to high temperatures.

* Corresponding author. Tel.: +61 395452259; fax: +61 395452448.
E-mail address: noel.clark@csiro.au (N.B. Clark).

0378-7753/$ – see front matter.
doi:10.1016/j.jpowsour.2009.06.054

Table 1
Metal oxidation potentials.

Metal	Oxidation potential E^o (V)
Au	−1.5
Ag	−0.8
Zn	0.76
Al	1.66
Mg	2.37

Milling to small particle sizes increases specific surface area and there by results in increased reactivity. Al, Mg and Zn all have positive oxidation potentials, whereas the noble metals Ag and Au have negative oxidation potentials (Table 1). Finely-ground Al, Mg and Zn rapidly oxidize in air, leading to an increase in the proportion of metal oxides present and decreased conductivity. Another issue is the potential safety hazard associated with reactive metals, particularly if the milling matrix is a volatile organic compound that could burn or explode. Based on these considerations, zinc is the obvious choice as a battery anode and has been used for this purpose for over 200 years [8].

The particle size that must be achieved is related to the intended printing technology. Screen print inks are generally high viscosity pastes capable of stabilising dispersions of large particles (tens of microns), whereas inkjet inks have much lower viscosity (typically of the order of 10 mPa s at the jetting temperature) so that particles must be much finer to pass through the printhead nozzles (<1 μm). Taken together, the lower viscosity and smaller particle sizes of inkjet inks make them more difficult to stabilise against agglomeration, so that loading concentrations must be reduced compared with screen print inks. Accordingly, screen print inks may be a much easier objective to attain than inkjet inks. Zinc dust is commercially available at particle sizes >60 μm and therefore may be suitable for screen print inks.

Printable electroactive zinc formulations have been patented by DuPont [9], based on a combination of Zn particles and a polymer binder such as polyhydroxy ether, polyurethane and/or a copolymer of acrylonitrile/vinylidene chloride dissolved in a suitable solvent system, with the optional addition of carbon as a conducting bridging agent. In the current study, this approach has been extended to formulations based on commercially available zinc and carbon, with polycarbonate dissolved in tetrahydrofuran as the binder. The objective is the preparation of galvanic metal inks for screen-printing or spray application, as these will have cost profiles appropriate for smart packaging applications. Further, a thin, zinc–air battery using electrocatalytic PEDOT printed on paper as the air-cathode has been prepared. The performance of this battery system is evaluated in relation to smart packaging applications.

2. Experimental

One litre of 0.1 M LiOH solution was prepared by dissolving 4.196 g $LiOH{\cdot}H_2O$ (Fluka USA) in deionised water. A 12 M solution of LiCl (Reagent Plus, Sigma–Aldrich, USA) was prepared by dissolving 25.43 g in 50 mL of the 0.1 M LiOH solution. An 8 M lithium chloride (LiCl) solution with a pH of 11 was prepared by dissolving 33.92 g of LiCl in 10 mL of 0.1 M LiOH and diluting to 100 mL in deionised water. A 1 M sodium chloride (NaCl) solution was prepared by dissolving 5.84 g NaCl (Merck; pro analysis, Germany) in deionised water to give 100 mL of solution. A solution of 100 mL of 1 M sulfuric acid (H_2SO_4) was prepared by diluting 10.22 g of concentrated H_2SO_4 (96% Pronalys; analytical reagent, Australia) with deionised water. A solution of 100 mL of 3 M potassium hydroxide KOH was prepared by dissolving 16.83 g KOH (Merck; pro analysis, Germany) in water. Absolute ethanol (Merck; GR for analysis ACS, Germany) was used without further purification.

For printing purposes, an aliquot of the LiCl/LiOH solution was mixed with molten (∼60 °C) polyethylene glycol (PEG, MW 1500, Huntsman Australia) in a 1:1 ratio by weight, to make 6 M LiCl. Ethanol or butan-1-ol was added to obtain a suitable viscosity for inkjet printing (*ca.* 10 mPa s) using a Dimatix Materials Printer (model 2811 FUJIFILM Dimatix, USA). To ensure sufficient coverage, eight layers of the electrolyte were printed on the substrate at a drop spacing of 20 μm and a cartridge temperature of 30 °C. On standing, the alcohol evaporated from the substrate and thereby caused the electrolyte to solidify within the sheet and return to the desired concentration. In other experiments, 8 M LiCl/LiOH electrolyte was formulated without the addition of PEG, and ethanol or butan-1-ol was added to lower the solution viscosity for inkjet printing.

Glossy photo paper (BP61GLP Brother, Japan), copy paper (Reflex, Australian Paper) and (EXPGreen50R Corporate Express, Australia), glass slides (Livingstone, Sigma–Aldrich, USA) and cotton plain weave textile (Spotlight, Australia) were used as test substrates, as indicated below. Conductive films composed of indium-tin-oxide on polyethylene naphthalate (ITO-PEN) were purchased from Peccell Technologies (Japan).

A uniform film of PEDOT was applied to the paper substrates by vapour phase polymerisation using methods described elsewhere [2]. Briefly, 6.5 mL of an oxidant solution composed of 40% iron(III)*p*-toluenesulfonate ($(Fe pTS)_3$) in butan-1-ol (marketed as Baytron C-B 40 by HC Starck, Singapore) was mixed with 0.15 g pyridine (BDH Australia), 1.86 g butan-1-ol and 0.05 g polyurethane diol (88 wt% in water, Sigma–Aldrich, Australia). This solution was passed through a polytetrafluoroethylene (PTFE) syringe filter with 0.5 μm pores and loaded into a new 1.5 mL DMC-11610 (10 pL nominal drop volume) cartridge of a Dimatix Materials Printer (model 2811 FUJIFILM Dimatix, USA). The solution was printed as 10 mm × 35 mm rectangles, with a 20 μm drop spacing and reservoir temperature of 30 °C, in four layers to ensure adequate coverage of the substrate. These settings gave an acceptable balance between print uniformity and edge resolution. Vapour phase polymerisation of PEDOT was then performed using the patterned oxidant–dye mixture as a template by simply exposing the dried substrate to EDOT monomer vapour at 60 °C for 30 min in a glass treatment vessel [10]. After polymerisation, the PEDOT was washed in ethanol for 30 min to remove Fe(II) and excess PTS, and then air dried. In similar manner, PEDOT|Au|Gore-Tex^{TM} air electrodes for the discharge measurements were prepared as detailed in a recent publication [4].

Zn–C–PC composites were prepared by mixing zinc (Merck; pro analysis, particle size >60 μm, Germany) and carbon powder (BDH, UK) in a 5 wt% solution of polycarbonate (PC, Sola International, Australia) in tetrahydrofuran (THF, Merck; LiChrosolv, Germany), to give a 15 wt% PC binder content with respect to the Zn–C mixture. The suspensions were ground using a mortar and pestle, to ensure homogeneity. The prepared suspensions were applied to substrates, which were equipped with a polymer mask (1 cm × 2 cm) by (i) using a pipette followed by drawing down the suspension with a glass rod, (ii) an air-brush (Paasche, USA) operating at 345 kPa at a distance of 150–200 mm; and (iii) using screen-printing equipment (Riso, Japan) and applying the suspension by means of a rubber blade. Films substituting zinc with copper (BDH, UK), silver (Merck; pro analysis, Germany) and silica gel 60 (Merck; for column chromatography, Germany) were prepared in an identical manner.

Prototype printed batteries were prepared as follows. A 10 mm × 20 mm rectangle of conductive PEDOT was applied to photo quality paper, as described above. A $Zn_{0.5}C_{0.5}PC_{0.15}$ film of corresponding size was applied to the underside of photo quality paper opposite the PEDOT coating. A LiCl/LiOH electrolyte solution was absorbed into the paper matrix. The two sides of the device were electrically connected and subjected to discharge measurements.

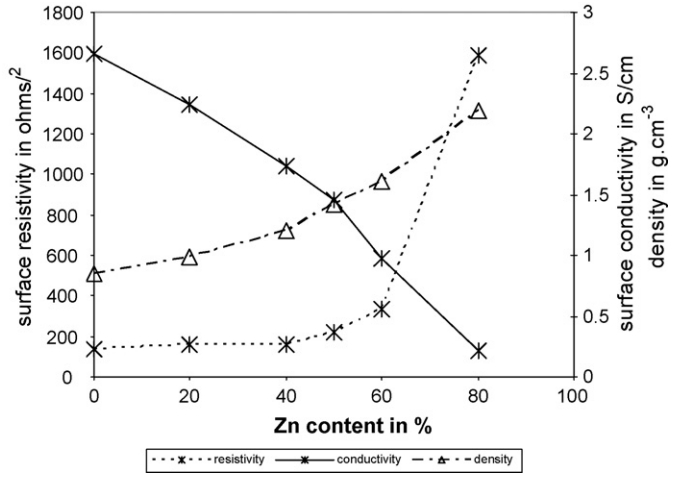

Fig. 1. Electrical surface properties of Zn/C/PC films for different Zn:C contents.

Surface resistivities (R_S) were measured using a 4-needle probe setup (Jandel RM3, USA) applying a current of 100 μA. These were then mathematically converted into surface conductivities G_S ($G_S = R_S^{-1}/d$; d = thickness). On carbon-sputtered samples, surface topography was determined with a Philips XL 30 Field Emission Scanning Electron Microscope. Secondary electron and backscattering electron images were recorded. Film thicknesses were determined with a Dektak 6M Stylus Profiler (Veeco USA) equipped with a BenchMate anti-vibration system from Kinetic Systems, USA. The stylus, which had a radius of 12.5 μm using a force of 10 mg, scanned the sample at a speed of 400 μm s^{-1}, and after levelling, the film thickness was determined using the average step height model (ash).

The performance of each device was determined with a NEWWARE battery testing unit in conjunction with BTS TestControl V5.1 software. The Zn films, applied to ITO-PEN substrates using the draw-down method, were electrically connected to a PEDOT:oxygen electrode and immersed in an electrolyte solution. The current flow was controlled to 500 μA and the generated voltage was measured over time until all of the available Zn was consumed; i.e., when the voltage dropped to zero. The efficiency was calculated from the ratio of the measured performance (expressed in Ah) to the theoretically expected performance, based on the amount of applied Zn.

3. Results and discussion

As noted above, Zn should have a sufficiently high oxidation potential to reduce inherently conducting polymers such as PEDOT or PPy. To prepare a zinc-based liquid formulation, a tetrahydrofuran (THF) solution of polycarbonate (PC) was chosen; PC is suitable as a binder due to its mechanical properties, availability and low price. Preliminary studies showed, however, that coatings composed of Zn and PC alone are not conductive. SEM images revealed that there was no physical contact between the Zn particles. Therefore, carbon was employed as an additional conductive component to act as a physical bridge to connect the isolated Zn particles in the PC film.

The surface conductivities and surface resistivities for $Zn_xC_{x-1}PC_{0.15}$ (x = 0.2, 0.4, 0.6, 0.8) films applied to glass substrates are presented in Fig. 1. Conductivity decreases with increasing Zn content. This is surprising given that the conductivity of Zn metal (166,000 S cm^{-1}) is much higher than that of carbon (610 S cm^{-1}). One possible explanation is that the Zn particles are covered with a thin, insulating layer of zinc oxide (ZnO).

A clearer insight is obtained from measurements conducted on similar films in which zinc is substituted with silver or copper. Although the conductivities of copper (596,000 S cm^{-1}) and silver (630,000 S cm^{-1}) are much higher than that of zinc, similar trends in electrical resistance are evident. Surface conductivity is independent of the nature of the particles added and therefore suggests that the conductivity of carbon is the dominating factor. By contrast, the metal particles contribute very little to coating conductivity, perhaps due to poor electrical contact associated with oxide layers on the metal particles. The trend is similar even if completely non-conductive powders such as silica are added to the film formulation, again supporting the above statement that the conductivity of carbon dominates electrical surface properties. The copper and

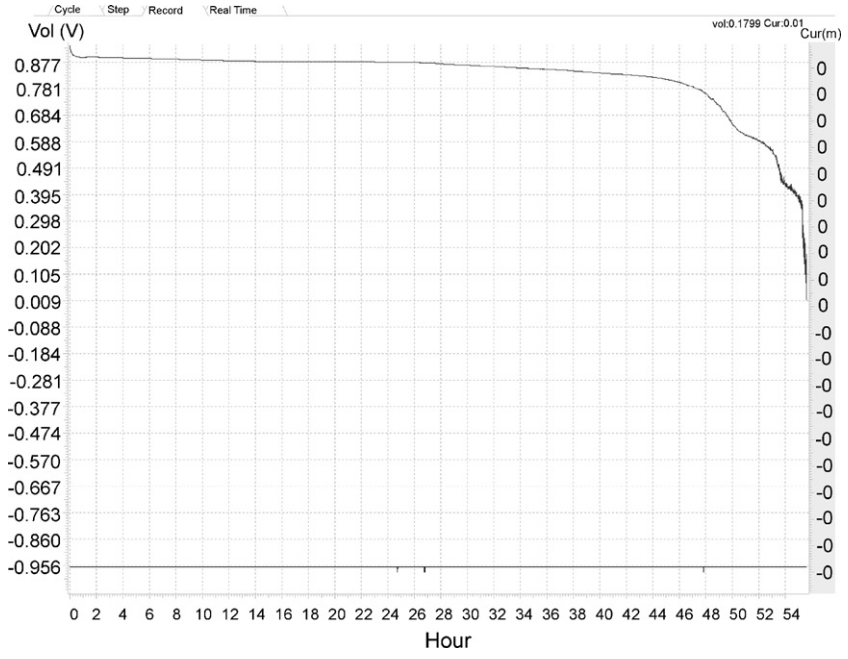

Fig. 2. Example of a discharge measurement. Voltage recorded at constant current for Zn/PEDOT:O_2 system. Voltage delivered is around 0.8 V over 2 days.

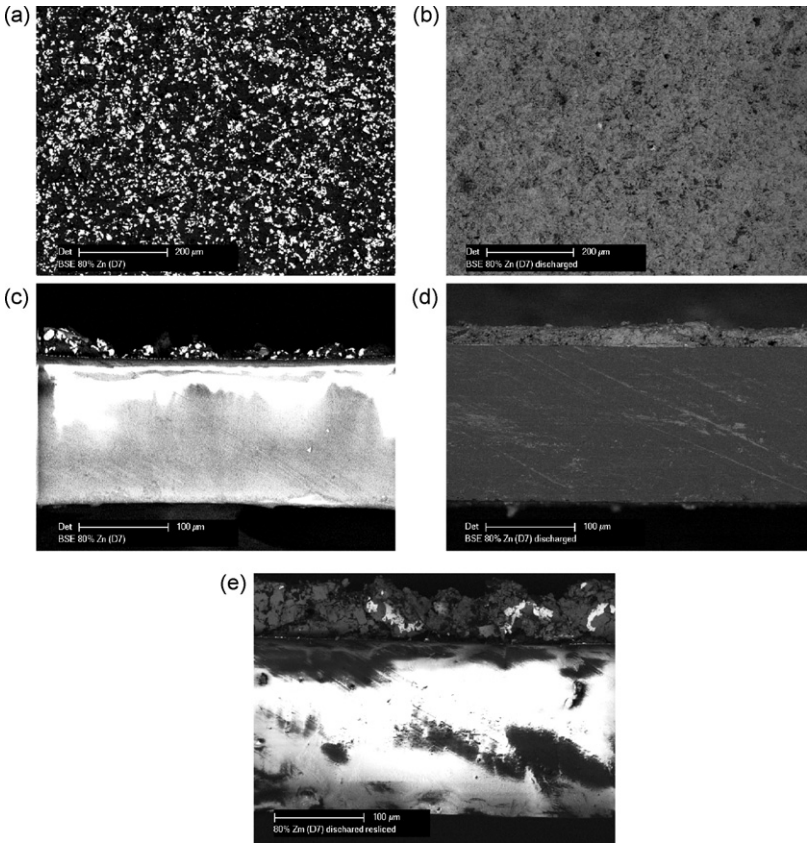

Fig. 3. BSE images of Zn/C/PC films before and after discharge: (a) surface before discharge, (b) surface after discharge, (c) cross-section before discharge, (d) cross-section after discharge, (e) cross-section further away from surface after discharge.

silica powders also have coarse particles that increase the variation in film thickness. This, in turn, increases the variability of the conductivity results, because film thickness is used in the calculation of surface conductivity from resistivity measurements. Conductivity also increases slightly with film thickness. This observation also supports the above explanation, as the denser Zn particles tend to settle towards the bottom of the film, thus adding less of their insulating properties to the measured surface conductivity.

To quantify performance (i.e., efficiency), discharge measurements were conducted (example shown in Fig. 2). Fig. 3 shows BSE images of a $Zn_{0.5}C_{0.5}PC_{0.15}$ film before and after being discharged in 1 M NaCl. It can be seen that the electrochemical reaction removes Zn from the surface. Taking a cross-section deeper into the sample, however, shows that there are still some Zn particles left inside the film. This means that although carbon effectively makes Zn available for the redox reaction, not all of the Zn is electrochemically converted. The electrolyte solution may be unable to penetrate deep into the film, making the inner Zn unavailable for electrochemical reaction.

The efficiencies for $Zn_xC_{1-x}PC_{0.15}$ ($x = 0.2$, 0.4, 0.6, 0.8) films in different electrolytes are shown in Fig. 4. There are three obvious trends. The results obtained in 1 M NaCl show that Zn-rich films (e.g., 80%) have lower efficiency. This may be related to the long measuring times that expose the samples to the aqueous electrolyte for several days and result in corrosive oxidation of the reactive base metal. Thus less metal is available to be electrochemically converted and the measured efficiencies are therefore lower. This conclusion is also in agreement with the second observation, which is that the efficiencies of Zn-rich films (e.g., above 50%) are higher in 8 M LiCl than in 1 M NaCl. Not only is the water content of LiCl much lower, but LiCl also binds water strongly. The LiCl electrolyte can therefore be considered as being mostly anhydrous, thus preventing the corrosive oxidation of Zn by water. The third trend can be seen in the LiCl series, where the conversion efficiencies are much higher for the Zn-rich samples. High Zn contents make the metal more easily accessible and are thus converted more easily. This increased accessibility of Zn is probably also the reason for the low efficiencies that are observed for the NaCl series and result in water oxidation for the 80% samples (e.g., lower efficiency).

Another factor affecting the measured efficiency in 1 M NaCl could be the formation of insoluble zinc oxo/hydroxo deposits, which could block the pore structure of the film, and thus prevent the inner, embedded Zn particles from participating in the reaction. Indeed, with the NaCl electrolyte, white, and insoluble precipitates in the electrolyte and deposition of the same material on the film

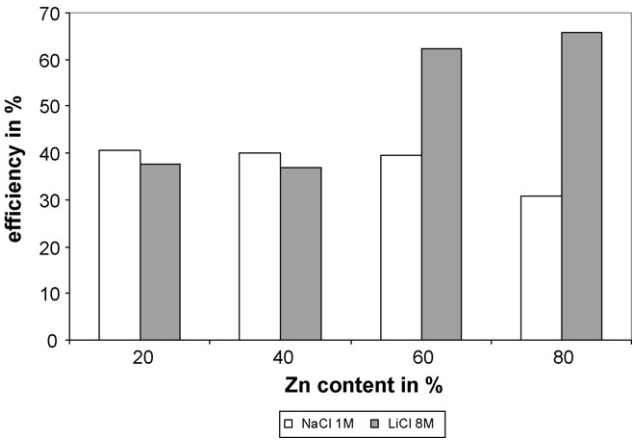

Fig. 4. Efficiencies dependent on Zn content in different electrolytes.

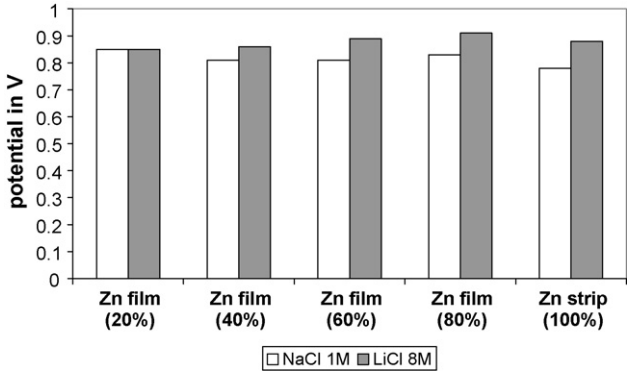

Fig. 5. Potential for Zn samples obtained in 1 M NaCl and 8 M LiCl at 250 μA cm^{-2}.

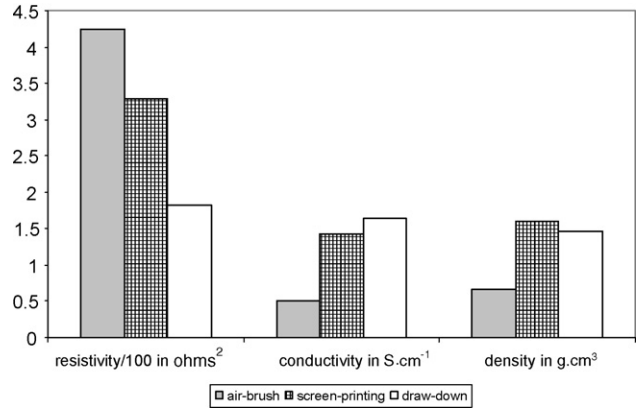

Fig. 6. Electrical surface properties and densities of $Zn_{0.5}C_{0.5}PC_{0.15}$ films applied by different methods.

after discharge are observed. On the other hand, soluble tetrahydroxozincate complexes, $[Zn(OH)_4]^{2-}$, are formed at the higher pH of the LiCi electrolyte and prevent blockage of the pore structure, so that the measured efficiency is increased.

The voltages generated by the Zn/C/PC systems are shown in Fig. 5. The potentials are similar and thus independent of the Zn content; even the electrolyte with strips of pure Zn foil produced the same voltage. The slight variations in the voltages are possibly caused by small changes in the experimental setup (e.g., distance between electrodes).

Returning to Fig. 4, the results show that efficiency is dependent on the type of electrolyte used. $Zn_{0.5}C_{0.5}PC_{0.15}$ films were applied by the draw-down method to several substrates including textiles, paper, glass and polymer, and then exposed to various electrolyte solutions such as 1 M NaCl, 8 M LiCl, ethanol, 1 M H_2SO_4 and 3 M KOH. Despite the fact that there are some adhesion problems between the glass and the coating, the films remained unchanged in NaCl, LiCl and ethanol.

Interestingly, the 1 M NaCl electrolyte solution turned cloudy after several days (probably from the formation of Zn oxidation products), whereas the ethanol and 8 M LiCl electrolyte solutions remained clear. These observations support the suggestion made earlier that whereas Zn becomes oxidised by water in the NaCl solution, this reaction is prevented by the high salt concentration of 8 M LiCl. Unsurprisingly, exposure to acid results in the liberation of hydrogen as a by-product of the reaction between zinc and acid. The other components of the films remain intact. Potassium hydroxide is the electrolyte that causes the most problems. After a couple of hours, the films start to tear and overnight they completely disintegrate. This is most extensive for those samples in which the composite suspension does not penetrate into the substrate (i.e., glass and paper). By contrast, the network structure of textiles provides a degree of physical protection from base attack, at least for a few hours. The films applied to polymer substrates have, however, remained remarkably unaffected even over a period of several weeks. In this case, the substrate is dissolved to some degree in the THF, thereby adding additional binder to the films and thus protecting and stabilising the films from base attack.

The dependence of the binder content and the film thickness of $Zn_{0.5}C_{0.5}PC_{0.15}$ composite films was also studied. Doubling the binder content does not seem to have a great effect on overall efficiency. The efficiency of thick films is, however, somewhat reduced. This suggests that Zn located deep inside thick films is unavailable for reaction. In addition, insoluble by-products produced from the oxidation of Zn further reduce efficiency by blocking pores in the film structure.

More important than the formulation composition is the method of application. Fig. 6 shows that the films applied by the previously discussed draw-down method and screen-printing techniques are similar with respect to their density and electrical properties, whereas the films applied with an air-brush have a lower density and much poorer conductivity. Similar trends are evident from the thickness profiles (Fig. 7), which show that the air-brushed films are of low density and have a rough surface. SEM investigations revealed that the air-brushed films have porous structures with many voids, presumably because THF (a low boiling point solvent) rapidly evaporates (Fig. 8).

The films obtained by applying formulations with a composition of $Zn_{0.5}C_{0.5}PC_{0.15}$ onto various substrates (paper, textile, glass, polymer) using different methods (draw-down, air-brush, screen-printing) are all conductive (Fig. 9). The measured resistivities (R_S) only provide a rough trend compared with the more quantitative surface conductivities (G_S). The latter, however, need to be calculated from the film thickness, which is difficult to determine or loses meaning if (i) the substrate is not even and smooth or (ii) if the sample penetrates into the substrate. This is also evident when comparing the surface resistivities of coatings applied to glass by the three application methods (Figs. 6 and 9). Despite different R_S values for identical systems, the calculations result in similar surface conductivities. Although care needs to be taken when comparing the results, it seems that the highest conductivity is achieved for smooth, non-porous substrates (e.g., glass).

Rectangles of conductive PEDOT were applied to photo-quality paper by inkjet printing an oxidant followed by vapour phase polymerisation (Fig. 10). The $Zn_{0.5}C_{0.5}PC_{0.15}$ film was applied to the underside of paper opposite to the PEDOT coating using an air-brush, and LiCl/LiOH electrolyte applied as a liquid that was

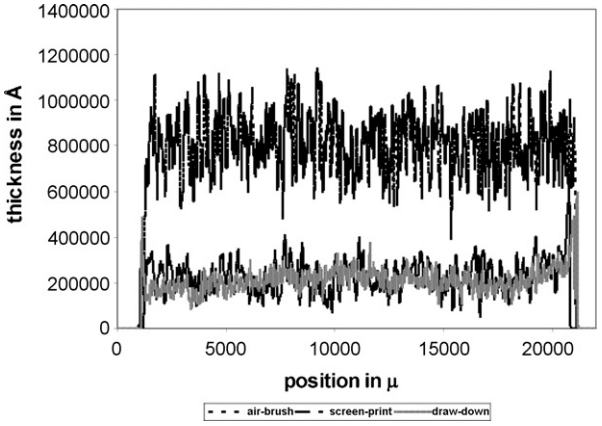

Fig. 7. Thickness profile of $Zn_{0.5}C_{0.5}PC_{0.15}$ films applied by different methods.

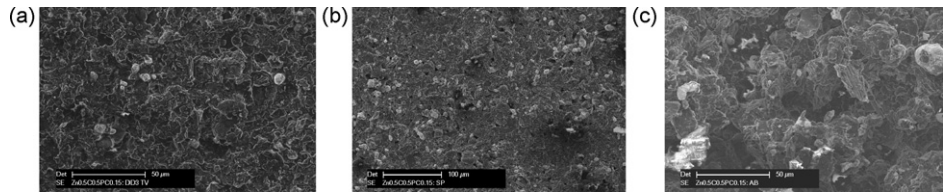

Fig. 8. Scanning electron micrographs of surface of $Zn_{0.5}C_{0.5}PC_{0.15}$ films obtained by (a) draw-down method, (b) screen-printing and (c) air-brushing.

absorbed into the paper matrix. The two sides were electrically connected and subjected to discharge measurements. The performance of these prototype batteries appears to be independent of the battery composition in terms of the amount of formulation, the Zn/C ratio and the electrolyte. The capacity measured for the paper-based prototypes (around 0.5 mAh cm^{-2}) is significantly lower than that obtained in the discharge experiments and indicates that the paper/electrolyte system may be limiting battery performance. Impedance measurements of the used paper battery show the electrical resistance to be in the 100 kΩ range, which suggests that the ionic mobility of the paper–electrolyte system significantly decreases during operation (initial resistance was in the 0.2 kΩ range). At this stage, it is not clear what part of the photo-paper structure causes this problem, and further work is planned to the optimise paper and/or electrolyte composition.

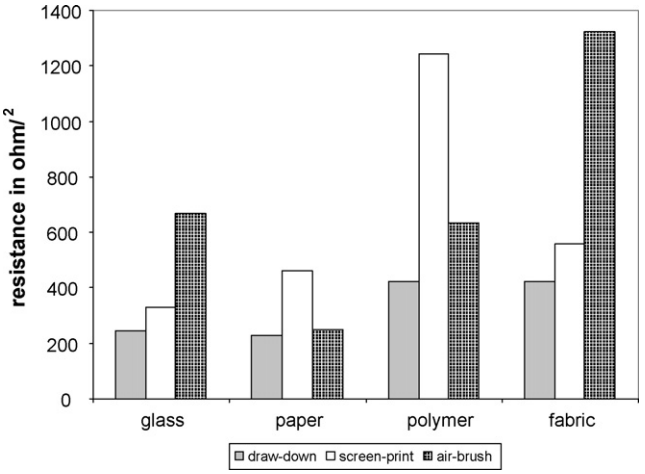

Fig. 9. Surface resistivity of $Zn_{0.5}C_{0.5}PC_{0.15}$ films on various substrates applied using different methods.

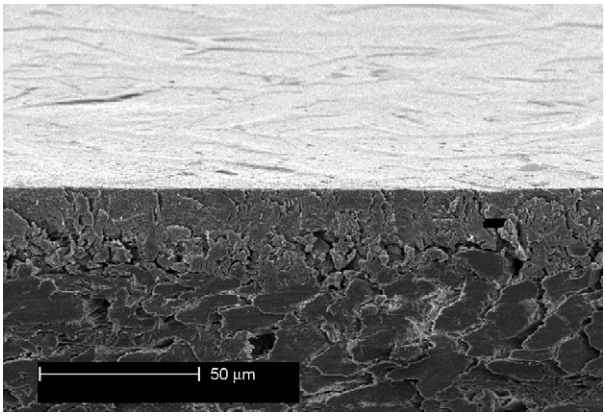

Fig. 10. SEM image of cross-section of photo-quality inkjet paper. VPP PEDOT absorbed into top 25 μm, apparent from change in texture.

4. Conclusions

$Zn_xC_{1-x}PC_{0.15}$ (with $x = 0.2$, 0.4, 0.6, 0.8) formulations have been prepared and applied to a range of substrates that included paper, glass, textiles and polymers using a pipette/draw-down method, air-brushing and screen-printing. The conductivity of the Zn/C/PC films decreases with increasing Zn content. This is probably associated with the insulating oxide layer surrounding the Zn particles. Conductivity is also higher for non-porous substrates such as sized paper and glass, compared with textiles and polymer substrates. Conductivity also increases with increasing film thickness.

Electrochemical efficiency was determined by discharge measurements. While efficiency is independent of the Zn content, it is highly dependent on the type of electrolyte. The efficiency is higher in 8 M LiCl (pH 11) compared with 1 M NaCl, probably because there is less water in the LiCl system, thus reducing aqueous zinc corrosion. The high pH also results in the dissolution of Zn-oxo precipitates that prevents blockage of the surrounding matrix and thus enhances efficiency. While the binder content has no effect, increasing film thickness decreases efficiency. This is due to the dense Zn particles settling to the bottom of the film and making them unavailable for electrochemical reaction. The generated potential, however, is independent of the Zn source, Zn content or the electrolyte.

The Zn/C/PC films are stable in the presence of likely electrolytes such as salt solutions and protonic solvents. Although acid reacted with the Zn, the general film structure remains unaffected. Strongly basic solutions result in complete disintegration of the films, with the exception of polymer substrates, where the dissolution of substrate by the THF solvent provided a protective binder to the composite. In contrast to the LiCl electrolyte, the Zn/C/PC films turn the NaCl electrolyte cloudy through the formation of Zn-oxo species that result from the reaction with water.

Applying the formulations using an air-brush give rise to in the formation of porous films, with poorer electronic properties (e.g., conductivity and conversion efficiency) compared with the denser films obtained through screen-printing or the draw-down method.

A printed battery prototype applied to photo-quality inkjet paper shows discharge characteristics slightly poorer than those obtained in discharge experiments conducted on the zinc composite applied to ITO-PEN substrates.

Acknowledgements

The SEM images were collected by Mark Greaves at CSIRO Materials Science and Engineering. The authors are indebted to Professors Douglas MacFarlane and Maria Forsyth of Monash University, Professor Gordon Wallace of the University of Wollongong, and Dr. Nafty Vanderhoek at CSIRO Materials Science and Engineering, for valuable discussions and suggestions. The work was financially supported by the ARC Centre of Excellence for Electromaterials Science and CSIRO Materials Science and Engineering.

References

[1] B. Winther-Jensen, N.B. Clark, R.J.N. Subramanian, S. Helmer, G. Ashraf, G. Wallace, L. Spiccia, D. MacFarlane, J. Appl. Polym. Sci. 104 (2007) 3938–3947.
[2] B. Winther-Jensen, N.B. Clark, React. Funct. Polym. 68 (2008) 742–750.
[3] G.G. Wallace, P.C. Innis, Aust. Prov. Pat. WO2007090232 (2007).
[4] B. Winther-Jensen, O. Winther-Jensen, M. Forsyth, D.R. MacFarlane, Science 321 (2008) 671–674.
[5] B. Winther-Jensen, M. Gaadingwe, D.R. MacFarlane, M. Forsyth, Electrochim. Acta 53 (2008) 5881–5884.
[6] R. Blake, Fuji Film Sericol, Personal communication (2007).
[7] S. Fletcher, University of Loughborough, personal communication (2007).
[8] X.G. Zhang, J. Power Sources 163 (2006) 591–597.
[9] J.R. Dorfman (Du Pont), US2004009398-A1 (2004).
[10] B. Winther-Jensen, J. Chen, K. West, G.G. Wallace, Macromolecules (2004) 5930–5935.